

# Experimental evidence for internal structure in aqueous–organic nanodroplets

Barbara E. Wyslouzil,<sup>\*ab</sup> Gerald Wilemski,<sup>c</sup> Reinhard Strey,<sup>d</sup> Christopher H. Heath<sup>b</sup> and Uta Dierregsweiler<sup>b</sup>

Received 19th October 2005, Accepted 11th November 2005

First published as an Advance Article on the web 21st November 2005

DOI: 10.1039/b514824c

The spatial distribution of species within an aerosol droplet influences how it interacts with its environment. Despite the ubiquity of multicomponent nanodroplets in natural and technological aerosols, there are no published measurements of their internal structure. Here, we report the first experimental results for structure in aqueous organic nanodroplets based on small angle neutron scattering by high number density aerosols. For H<sub>2</sub>O–n-butanol droplets, fitting of the diffraction patterns confirms the picture of an aqueous core containing ~3 mol% alcohol covered by a shell of densely packed alcohol molecules.

Internal structure substantially affects the heterogeneous reactions, the growth and evaporation kinetics, the accommodation of trace gas species, and the radiative properties of droplets.<sup>1,2</sup> Furthermore, the rate at which new particles form is sensitive to the surface free energy, and thus, to the composition and structure of the nanometre sized critical clusters.<sup>3</sup> Evidence for structure in nanodroplets includes the partitioning of ethanol to the surface of ethanol–water clusters in Monte Carlo<sup>3</sup> and molecular dynamics simulations<sup>4</sup> and the scaling with size observed for the organic carbon content in atmospheric aerosols.<sup>5</sup> Direct experimental evidence for a core–shell structure in nanodroplets, however, has been lacking until now.

To investigate nanodroplet structure, we developed *in situ* small angle neutron scattering (SANS) experiments to study aerosols with droplet or particulate radii in the range 1–20 nm.<sup>6,7</sup> With wavelengths between 0.5 and 2 nm, cold neutrons are well suited to probe the structure of matter on this length scale.<sup>8</sup> Our experimental approach parallels the contrast matching technique used to investigate the structure of micro-emulsions.<sup>9</sup> As Fig. 1 illustrates for a core–shell model, selective deuteration changes both the shape and intensity of the scattering spectrum. Deuterated compounds coherently scatter neutrons more intensely than their hydrogenated analogues, and, thus, for the H<sub>2</sub>O–deuterated n-butanol (d-butanol) aerosol, scattering comes primarily from the organic rich shell of the droplets. In contrast, scattering from the D<sub>2</sub>O–

hydrogenated n-butanol (h-butanol) aerosol comes almost exclusively from the aqueous core. The key differences between the two curves include more intense scattering from the D<sub>2</sub>O core at low  $q$ , a pronounced feature in the shell scattering case at intermediate  $q$ , and a difference in the rate of decrease in scattering intensity,  $q^{-4}$  vs.  $q^{-2}$ , at high  $q$ . For the real H<sub>2</sub>O–d-butanol aerosol, the feature at intermediate  $q$  will be less pronounced because of isotopic exchange of the labile D of the alcohol with H from water and because of the moderate solubility of the deuterated alcohol in the aqueous core.

Our aerosols are formed by nucleation and condensation of the targeted species from a dilute vapour–N<sub>2</sub> carrier gas mixture as it flows through a supersonic nozzle.<sup>10</sup> The number densities of droplets  $N$  are typically between 10<sup>11</sup> and 10<sup>12</sup> cm<sup>-3</sup>. For an average droplet radius  $\langle r \rangle$  of 10 nm, the volume fraction  $\phi$  is  $\sim 5 \times 10^{-6}$ , and the absolute scattering intensities

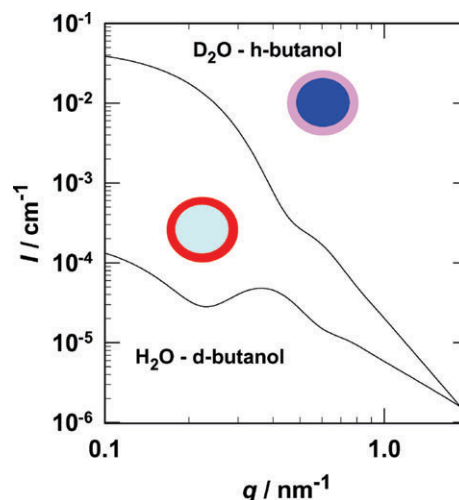


**Fig. 1** The aerosols consist of multicomponent droplets suspended in N<sub>2</sub> carrier gas. The colour coding for the droplet cartoons is: red (pink) = hydrocarbon with positive (negative) scattering length density, dark blue (light blue) = water with positive (negative) scattering length density. The lower curve corresponds to the expected scattering signal from droplets with a pure H<sub>2</sub>O core and a pure d-butanol shell, while the upper curve corresponds to droplets with a pure D<sub>2</sub>O core and a pure h-butanol shell. The calculations assumed a polydisperse (Schultz) distribution of cores and a constant shell thickness with:  $\phi = 3 \times 10^{-6}$ ;  $\langle r_{\text{core}} \rangle = 9$  nm; core polydispersity, 0.2;  $\delta_{\text{shell}} = 0.5$  nm. The scattering length densities are: d-butanol =  $6.51 \times 10^{-6}$  Å<sup>-2</sup>, D<sub>2</sub>O =  $6.39 \times 10^{-6}$  Å<sup>-2</sup>, h-butanol =  $-3.29 \times 10^{-7}$  Å<sup>-2</sup>, H<sub>2</sub>O =  $-5.60 \times 10^{-7}$  Å<sup>-2</sup>.

<sup>a</sup> Chemical and Biomolecular Engineering Department, The Ohio State University, Columbus, OH 43210, USA. E-mail: wyslouzil.1@osu.edu

<sup>b</sup> Chemical Engineering Department, Worcester Polytechnic Institute, Worcester, MA 01609, USA

<sup>c</sup> Department of Physics, University of Missouri – Rolla, Rolla, MO 65409, USA

<sup>d</sup> Institut für Physikalische Chemie, Universität zu Köln, D-50939 Köln, Germany

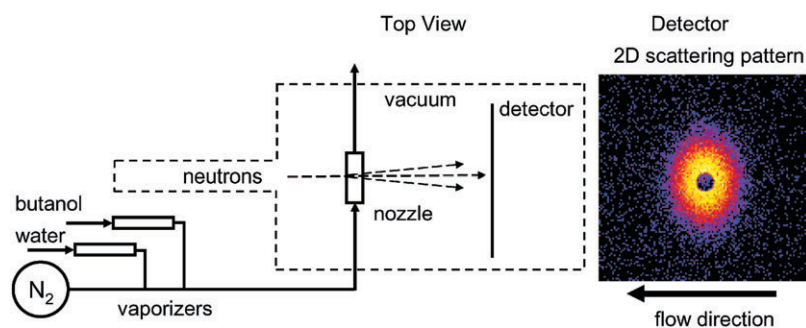


**Fig. 2** (left) A schematic diagram of the experimental apparatus illustrating the material flows and the crossed beam scattering geometry. During a SANS experiment the windows that separate the sample box from the neutron pre-sample flight path and the detector tube are removed, and the neutron flight path is evacuated to both minimize and stabilize the background scattering. (right) A 2D scattering pattern illustrates the distortion that arises because the ratio of the particle to neutron velocities in this experiment is  $\sim 0.9$ . The dark central region is due to the beam stop. The scattered neutron intensity scale ranges from yellow (highest) to black (lowest). The aerosol flow is from right to left in the horizontal plane.

are approximately four orders of magnitude lower than those of typical microemulsions.

Fig. 2 is a sketch of the experimental system. For the current experiments, the pressure and temperature at the entrance to the nozzle were 60.0 kPa and 308.15 K, respectively. The flow rate of  $N_2$  carrier gas was  $\sim 17$  mol/min while the condensable flow rate was 0.355 mol/min for the  $H_2O$ -d-butanol aerosol and 0.305 mol  $min^{-1}$  for the  $D_2O$ -h-butanol. In both experiments, the initial condensable vapor contained 6.2 mol% butanol. At 298 K the concentration of butanol in the saturated water-rich phase is only  $\sim 2$  mol%,<sup>11</sup> and, thus, we must produce and mix two vapour streams to generate the desired composition. In earlier experiments using propanol and water, we found no differences in condensation behaviour if the desired mixture was vaporized directly or if two vapour streams were produced independently.<sup>12</sup>

The neutron scattering experiments were carried out using the NG7 SANS instrument at NIST. The nozzle and associated plumbing were placed in the sample box with the neutron beam perpendicular to the flow in the nozzle. The nozzle sidewalls have 0.45 mm thick silicon windows that are transparent to the neutrons and separate the flow inside the nozzle from the evacuated sample chamber. The neutron wavelength was  $\lambda = 0.8$  nm with a wavelength spread of  $\Delta\lambda/\lambda = 0.22$ . Measurements of scattered intensity from the aerosol and from the background (pure  $N_2$  gas) were made in alternating 30 min intervals to ensure the background did not drift. The total sample integration time for the  $H_2O$ -d-butanol aerosol was 135 min at a sample to detector distance (SDD) of 2 m. For the  $D_2O$ -h-butanol aerosol it was 60 minutes at each SDD (2.0 m and 3.75 m). Longer background integrations, 8 h at 2 m and 9 h at 3.75 m, were obtained by combining the local background with that measured during other experiments conducted during the same NIST visit. In the scattering volume, the droplet/gas velocity was  $\sim 450$  m  $s^{-1}$ , and the gas pressure and temperature were  $\sim 17$  kPa and 235 K, respectively. Thus, the temperature is well above the 200 K limit that Bartell<sup>13</sup> and co-workers found was required to freeze pure water droplets in this size range and under comparable flow conditions.

One interesting complication in our experiments is the Doppler shifted scattering patterns that arise because the high

speed droplets and the neutrons ( $500$  m  $s^{-1}$ ) intersect at a right angle (Fig. 2). Thus, neutrons scattered in the direction of the aerosol beam acquire an added momentum shift that systematically distorts the two-dimensional scattering patterns measured in the laboratory frame. In earlier work we explored this phenomenon in detail<sup>14,15</sup> and developed a Doppler correction procedure that is implemented in the SANS data reduction program.<sup>16</sup>

Fig. 3a illustrates the SANS scattering spectra measured for the two aqueous-butanol nanodroplet aerosols. The data were reduced following the procedure outlined in Kim *et al.*<sup>10</sup> and setting the droplet velocity equal to the gas velocity derived from axial pressure measurements. The spectrum corresponding to the  $H_2O$ -d-butanol aerosol clearly contains the key features associated with scattering from a core-shell structure, while the corresponding spectrum from the  $D_2O$ -h-butanol aerosol looks like scattering from a polydisperse distribution of spheres.

To derive the structural parameters of the droplets and their overall composition, we used the NIST data analysis programs<sup>16</sup> to fit the  $H_2O$ -deuterated n-butanol spectrum assuming a polydisperse (Schultz) distribution of cores ( $r_{core}$ ) covered by a layer of alcohol with constant thickness  $\delta$ . Because the volume fraction of the aerosol  $\phi$  and the scattering length densities of the core ( $SLD_{core}$ ) and shell ( $SLD_{shell}$ ) are perfectly correlated, only one of these parameters can be varied. Thus, we set  $\phi$  equal to the value determined by the pressure trace measurements, and set  $SLD_{shell}$  equal to  $SLD_{d-butanol}$  ( $C_4D_9OH_{0.97}D_{0.03}$  to account for H-D exchange with  $H_2O$ ). The fitting procedure returned the average radius, polydispersity, and scattering length density of the droplet core, the thickness of the shell, and the magnitude of the constant scattering from the background. To test for the presence of  $H_2O$  in the shell, we decreased  $SLD_{shell}$  and refit the spectrum. Decreasing  $SLD_{shell}$  always made the fit of the model to the measured scattering intensity worse as estimated by a  $\chi^2$  statistic. The best fit parameters are given in Table 1 and the solid line in Fig. 3b is the fit.

To test the consistency of the fit, we used the  $SLD_{core}$  returned by the fit to estimate the composition of the core and found that the mole fraction of butanol in the core was  $x_{core} = 0.029$ . Solubility measurements for butanol in water

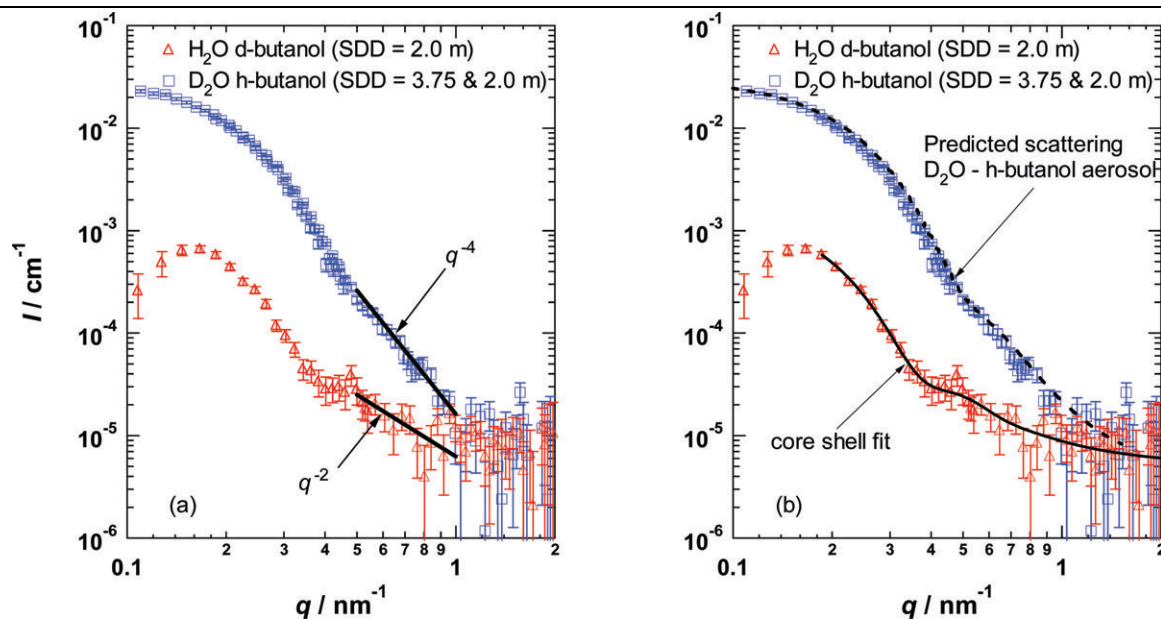


**Fig. 3** Scattering from a D<sub>2</sub>O–h-butanol aerosol is compared to that from a H<sub>2</sub>O–d-butanol aerosol formed under identical conditions ( $T$ ,  $p$ , mol% butanol) in the nozzle. SDD is the sample-to-detector distance. The falloff in intensity at low  $q$  is due to shadowing from the beam stop. (a) In the high  $q$  region, the intensity falls off as  $q^{-4}$  for the D<sub>2</sub>O-rich droplets, but only as  $q^{-2}$  for the H<sub>2</sub>O-rich droplets. The residual background ( $\sim 5 \times 10^{-6} \text{ cm}^{-1}$ ) arises primarily from incoherent scattering from hydrogen species (b) A well mixed droplet model (not shown) cannot reproduce the feature in the region  $0.4 \text{ nm}^{-1} < q < 0.5 \text{ nm}^{-1}$  of the H<sub>2</sub>O–d-butanol spectrum. A core shell model fits the data well ( $\chi^2/(\text{degrees of freedom}) \approx 0.8$ ). After adjusting the parameters from the core–shell fit to account for the differences in scattering length density and molar flow rates of the condensable material (see text for further details), the scattering spectrum for the D<sub>2</sub>O–h-butanol aerosol is *predicted* rather well.

are not available at low temperatures, but the limiting concentration at 273 K is 2.7 mol%, and below about 325 K solubility increases with decreasing temperature.<sup>11</sup> Thus, our fit value for  $x_{\text{core}}$  is quite reasonable. We then used the structural parameters and compositions to determine the amount of H<sub>2</sub>O and d-butanol contained in the aerosol. The volume fraction of d-butanol in the aerosol predicted by the core–shell droplet model (22%) differed by only 12% from that entering the nozzle (25%). The volumetric flow rate of either component was less than that entering the nozzle—consistent with our estimate that  $\sim 80\%$  of the vapor entering the nozzle condenses.<sup>17</sup>

A second consistency test relies on the observation that if the core–shell model and the parameters determined by fitting the H<sub>2</sub>O–d-butanol aerosol are reasonable, we should also be able to *predict* the scattering spectrum observed for the D<sub>2</sub>O–h-butanol aerosol by using these parameters, inverting the roles of D and H, and adjusting the average droplet size<sup>18</sup> for the slightly lower volumetric flows  $\dot{V}$  as  $\langle r_{\text{core,new}} \rangle = \langle r_{\text{core,old}} \rangle (\dot{V}_{\text{new}}/\dot{V}_{\text{old}})^{1/3}$ . The prediction is the dashed line passing through the D<sub>2</sub>O–h-butanol data (Fig. 3b). The remarkable consistency observed is strong support for the reliability and quality of our experimental procedures as well

as for our theoretical analysis of the results. Finally, from the volume fraction and structural information we determined that the number densities of the two aerosols are  $\sim 8 \times 10^{11} \text{ cm}^{-3}$ , typical of aerosols formed in this nozzle.

Our results have important implications for understanding the structure and behavior of nano-sized atmospheric droplets in situations ranging from marine aerosol evolution to cloud formation.<sup>1</sup> For example, they support the “inverted micelle” picture that has been invoked to explain the scaling of the carbon content of atmospheric aerosols with size.<sup>5</sup> They also demonstrate the strength of the *aerosol* SANS technique to probe samples under conditions of high metastability, low temperature, high pressure, or extreme cleanliness. These conditions, which are often difficult, if not impossible to achieve for bulk samples, are either the direct outcome of the nozzle expansion or, in the case of high pressure, the result of the Laplace effect in droplets of small radius.

We also find it interesting that, although our measurements probe very small length scales at subcooled conditions, our results on structured nanodroplets can be qualitatively understood in terms of the behavior of macroscopic systems at room temperature. The interfacial shell of the water-rich droplets resembles the vapor–liquid interface of the water-rich phase of

**Table 1** The structural parameters for H<sub>2</sub>O–d-butanol derived by fitting the SANS spectrum. Values without uncertainties have been assigned as described in the text. For the D<sub>2</sub>O–h-butanol aerosol,  $\phi$  comes from the pressure trace experiment,  $\langle r_{\text{core}} \rangle$  has been scaled to account for the difference in  $\phi$ , the scattering length densities are adjusted by inverting the role of H and D while maintaining the shell and core compositions, and the remaining parameters are identical to those derived from the H<sub>2</sub>O–d-butanol fit

Aerosol	$\phi$	$\langle r_{\text{core}} \rangle / \text{nm}$	$\sigma / r$	$\delta / \text{nm}$	$\text{SLD}_{\text{core}} / \text{\AA}^{-2}$	$\text{SLD}_{\text{shell}} / \text{\AA}^{-2}$	Background/ $\text{cm}^{-1}$
H <sub>2</sub> O–d-butanol	$3.4 \times 10^{-6}$	$9.06 \pm 0.39$	$0.197 \pm 0.047$	$0.42 \pm 0.05$	$4.57 \times 10^{-7} \pm 0.69 \times 10^{-7}$	$5.84 \times 10^{-6}$	$5.25 \times 10^{-6} \pm 1.03 \times 10^{-6}$
D <sub>2</sub> O–h-butanol	$2.9 \times 10^{-6}$	8.65	0.197	0.42	$5.43 \times 10^{-6}$	$3.55 \times 10^{-7}$	$5.25 \times 10^{-6}$

bulk aqueous butanol mixtures, which is highly enriched in butanol.<sup>19,20</sup> The thickness of the shell (0.4 nm) is comparable to the interfacial peak width for the hydrophobic tail group found in Monte Carlo simulations (0.8 nm) of the bulk interface.<sup>20</sup> Furthermore, the limited size of the droplets means that these experiments are unlikely to be contaminated by capillary wave roughness that can be an issue in reflectivity measurements of interfacial thickness.<sup>20,21</sup> Finally, the high concentration of butanol in the interfacial zone is a microscopic precursor of the butanol-rich phase on the other side of the miscibility gap. This suggests that in a butanol-rich vapor the nanodroplet structure should resemble that of the bulk butanol-rich phase. How the structure of these droplets changes as the vapor composition is shifted from water-rich to butanol-rich and whether or not bulk thermodynamics can predict such a transition stand as interesting questions for future research.

## Acknowledgements

We acknowledge the support of the National Institute of Standards and Technology, Department of Commerce, in providing the neutron research facilities used in this work. We thank J. Barker and C. Glinka at the NCNR for their continued help and support, and J. Cheung and J. Wölk for help developing the techniques and conducting preliminary experiments. This work was supported by grants from the National Science Foundation (B.E.W.), the Engineering Physics Program of DOE-BES (G.W.), the Deutsche Forschungsgesellschaft (R.S.) and NATO (to B.E.W., G.W. and R.S.).

## References

- 1 Y. Rudich, *Chem. Rev.*, 2003, **103**, 5097.
- 2 T. L. Eliason, J. B. Gilman and V. Vaida, *Atmos. Environ.*, 2004, **38**, 1367.
- 3 B. Chen, J. I. Siepmann and M. L. Klein, *J. Am. Chem. Soc.*, 2003, **125**, 3113.
- 4 M. Tarek and M. L. Klein, *J. Phys. Chem. A.*, 1997, **101**, 8639.
- 5 G. B. Ellison, A. F. Tuck and V. Vaida, *J. Geophys. Res. D.*, 1999, **104**, 11633.
- 6 B. E. Wyslouzil, J. L. Cheung, G. Wilemski and R. Strey, *Phys. Rev. Lett.*, 1997, **79**, 431.
- 7 H. Wang, B. Zhao, B. E. Wyslouzil and K. Streletzky, *Proc. Combust. Inst.*, 2003, **29**, 2749.
- 8 *Structure and Dynamics of Strongly Interacting Colloids and Supramolecular Aggregates in Solution*, ed. S.-H. Chen, J. S. Huang and P. Tartaglia, NATO ASI Series C: Mathematical and Physical Sciences, Kluwer, Amsterdam, vol. **369**, 1992.
- 9 M. Gradzielski, D. Langevin, L. Magid and R. Strey, *J. Phys. Chem.*, 1995, **99**, 13232.
- 10 Y. J. Kim, B. E. Wyslouzil, G. Wilemski, J. Wölk and R. Strey, *J. Phys. Chem. A*, 2004, **108**, 4365.
- 11 A. F. M. Barton, *Solubility Data Series Alcohols with Water*, Pergamon, New York, vol. **15**, 1984.
- 12 B. E. Wyslouzil, C. H. Heath, J. L. Cheung and G. Wilemski, *J. Chem. Phys.*, 2000, **113**, 7319.
- 13 L. S. Bartell, *Annu. Rev. Phys. Chem.*, 1998, **49**, 43.
- 14 B. E. Wyslouzil, G. Wilemski, J. L. Cheung, R. Strey and J. Barker, *Phys. Rev. E.*, 1999, **60**, 4330.
- 15 G. Wilemski, *Phys. Rev. E*, 2000, **61**, 557.
- 16 *NG3 and NG7 30-meter SANS Instruments Data Analysis Manual*, National Institute of Standards and Technology, NIST NCNR, Gaithersburg, MD, 2001, [www.ncnr.nist.gov/programs/sans/manuals/data\\_anal.html](http://www.ncnr.nist.gov/programs/sans/manuals/data_anal.html).
- 17 S. Tanimura, Y. Zvinevich, B. E. Wyslouzil, M. Zahniser, J. Shorter, D. Nelson and B. McManus, *J. Chem. Phys.*, 2005, **122**, 194304.
- 18 In an earlier paper C. H. Heath, K. A. Streletzky, B. E. Wyslouzil, J. Wölk and R. Strey, *J. Chem. Phys.*, 2003, **118**, 5465, we found that scaling the radius of the droplets to account for differences in the volumetric flow rate predicts the change in the scattering intensity as  $q \rightarrow 0$ ,  $I_0$ , rather well where  $I_0 \propto N(r^6)$ .
- 19 Z. X. Li, J. R. Lu, R. K. Thomas, A. R. Rennie and J. Penfold, *J. Chem. Soc., Faraday Trans.*, 1996, **92**, 565.
- 20 B. Chen, J. I. Siepmann and M. L. Klein, *J. Am. Chem. Soc.*, 2002, **124**, 12232.
- 21 D. K. Schwartz, M. L. Schlossman, G. J. Kawamoto, P. S. Pershan and B. M. Ocko, *Phys. Rev. A*, 1990, **41**, 5687.